Mon. Not. R. Astron. Soc. **000**, 1–6 (2013) Printed 26 February 2024 (MN LATEX style file v2.2)

Metallicity bias in the kinematics of the Milky Way stellar halo

P. R. Kafle ⋆, S. Sharma, G. F. Lewis and J. Bland-Hawthorn
Sydney Institute for Astronomy, School of Physics, A28, The University of Sydney, NSW 2006, Australia

arXiv:1212.4576v2 [astro-ph.GA] 10 Feb 2013

Accepted 2013 January 14. Received 2013 January 13; in original form 2012 December 4

ABSTRACT
Here we study the metallicity bias in the radial and tangential velocity dispersions, the derived quantity called anisotropy and the mean azimuthal velocity profiles of the Milky Way stellar halo using Blue Horizontal Branch (BHB) stars taken from *SDSS/SEGUE* survey. The comparatively metal-rich sample ([Fe/H] > -2) has prograde motion and is found to have an offset of 40 km s^{-1} in the mean azimuthal velocity with respect to a metal-poor sample ([Fe/H] $\leqslant -2$) which has retrograde motion. The difference in rotation between the most metal-poor and most metal-rich population was found to be around 65 km s^{-1}. For galactocentric distances $r \lesssim 16$ kpc, an offset in velocity dispersion profiles and anisotropy can also be seen. In the inner regions, the metal-poor population is in average tangential; however, anisotropy is found to decrease monotonically with radius independent of metallicity. Beyond $r = 16$ kpc, both the metal-rich and the metal-poor samples are found to have tangential motion. The metallicity bias in the kinematics of the halo stars qualitatively supports the coexistence of at least two-components in the halo having different formation history e.g. in-situ formation and formation by accretion.

Key words: Galaxy: stellar content - Galaxy: halo - Galaxy kinematics: stars: horizontal-branch - stars: abundances

1 INTRODUCTION

The stellar halo is an excellent resource for testing theories of galaxy formation (Freeman & Bland-Hawthorn 2002; Helmi 2008). With the advent of new high quality surveys involving hundreds of thousands of stars, understanding the formation of the halo has become even more challenging. Under the ΛCDM paradigm of hierarchical formation, the stellar halo is thought to have been produced in part by accretion of satellite galaxies. Observational evidence for this comes from the detection of tidal streams and substructures in the halo of both the Milky Way and M31 (e.g., Majewski 1993; Ibata et al. 1995; Belokurov et al. 2006). Quantitative comparison of the amount of substructure and its physical properties seen in simulations with that of observations reveals broad agreement with the accretion theory (Bell et al. 2008; Starkenburg et al. 2009; Gilbert et al. 2009; Xue et al. 2011; Sharma et al. 2011b). Recent cosmological simulations (e.g., Zolotov et al. 2009; Font et al. 2011; McCarthy et al. 2012; Tissera et al. 2012) including star formation and feedback suggest that the inner regions of the halo might be dominated by in-situ component which have chemical and kinematic properties different from that of the accreted component. The kinematic and spatial distributions of the in-situ component is thought to resemble that of the disk–flattening and net prograde rotation.

Recent observational results also seem to suggest the need for an in-situ component. In their seminal paper, Carollo et al. (2007, hereafter C07) claim that the inner-halo component ($r < 15$ kpc) is comparatively metal-rich, has a prograde motion (0-50 km s^{-1}), with a slightly flattened spatial distribution and with stars on mostly radial orbits. In contrast, the outer-halo is comparatively metal-poor, has a strong retrograde motion (40-70 km s^{-1}), has a nearly spherical spatial distribution, with stars on a wide range of orbital eccentricities. These results were derived using stars in the Solar neighborhood which were roughly divided into inner and outer regions based on the maximum distance from the galactic plane reached by individual stellar orbits. Their analysis requires the use of proper motions for which it is important to have accurate distances. The impact of distance errors on the retrograde signature has been debated, e.g. see Schönrich et al. (2011) and Beers et al. (2012). A cleaner distinction between the inner and outer regions can only be done by taking a sample of stars which has much wider spatial distribution. This was done by Deason et al. (2011a) using BHB stars grouped into four regions in metallicity and distance spaces. Their results are in qualitative agreement with C07 and Carollo et al. (2010), i.e., the metal-rich population is prograde while the metal-poor population is retrograde. However, they find that stars between 15-25 kpc are on circular orbits while those beyond 25 kpc are on radial orbits. The derived quantity called anisotropy (Binney & Tremaine 2008) defined as

$$\beta = 1 - \frac{\sigma_\theta^2 + \sigma_\phi^2}{2\sigma_r^2} \quad (1)$$

describes the nature of the orbits, where σ_r, σ_θ, and σ_ϕ are radial, polar and azimuthal velocity dispersions respectively. Negative and

⋆ E-mail: p.kafle@physics.usyd.edu.au

© 2013 RAS

positive values of the anisotropy corresponds to the tangential and radial dominance of the orbits respectively. The arbitrary distance ranges make it difficult to compare the β results of BHB stars with those of C07. An arbitrary cut-off in metallicity ([Fe/H] $= -2$) was used to group the stars. In our recent work (Kafle et al. 2012, hereafter K12), we study β as a function of radius in greater detail and we show that the profile is not a simple monotonic function. We find that for $r < 15$ kpc, stars are on radial orbits; at larger radii, there is a sharp drop in β with a minimum of $\beta \approx -1.2$ at 17 kpc; beyond 20 kpc, β rises slightly. Given the complex variation of β with radius, it is important to study the radial profile of β and $v_{\rm rot}$ for different metallicities.

This paper is organized as follows. In Section 2, we discuss the theoretical aspect of our analysis, and the data being used. Section 3 presents our result about the metallicity biases in the kinematical profiles, $\sigma_r(r), \sigma_\theta(r), \sigma_\phi(r)$, $\beta(r)$, $v_{\rm rot}(r)$, of the Milky Way stellar halo. In Section 4, we conclude our result and describe the implications of the biases for the formation of the halo.

2 THEORY AND ANALYSIS

2.1 Distribution Function and Parameter estimation

Our main aim is to estimate the rotational velocity and the velocity dispersion as a function of radius. To do this we model the velocities using the Gaussian Velocity Ellipsoidal distribution function (GVE DF). A GVE DF with rotation about z-axis is given by

$$f(r,\mathbf{v}) = \frac{\rho(r)}{(2\pi)^{3/2}\sigma_r\sigma_\theta\sigma_\phi}\exp\left[-\frac{1}{2}\left(\frac{v_r^2}{\sigma_r^2}+\frac{v_\theta^2}{\sigma_\theta^2}+\frac{(v_\phi-v_{\rm rot})^2}{\sigma_\phi^2}\right)\right], \quad (2)$$

where $v_{\rm rot}$ is the mean azimuthal velocity. A GVE DF has been used in the context of the stellar halo to estimate the rotation (Frenk & White 1980) and the velocity dispersions (Sirko et al. 2004b; Smith et al. 2009b; Kafle et al. 2012). In their studies of halo subdwarf stars, Smith et al. (2009a) and Bond et al. (2010) have found that the tilt of the velocity ellipsoid is small and consistent with zero, and is therefore ignored in this analysis.

Ideally, we would like to know the full six-dimensional phase-space information of an individual halo star. But presently the proper motion information of the stars in the stellar halo beyond the Solar neighborhood ($r \gtrsim 10$ kpc) is not accurate enough to properly constrain the tangential motions. We thus resort to the line-of-sight component of the velocity and marginalize the DF over the two unknown components of the velocity (v_l, v_b). The marginalized DF can be expressed as,

$$F(l,b,d,v_{\rm los}|\sigma_r,\sigma_\theta,\sigma_\phi,v_{\rm rot}) = \iint f(r,\mathbf{v})dv_l dv_b. \quad (3)$$

Note the marginalization is over the tangential components of the velocities (v_l, v_b) in the heliocentric rest frame, whereas DF (Equation 2) is expressed in the galactocentric frame of reference. For the transformation between these reference frames, we assume the IAU adopted values of the Sun-Galactic centre to be 8.5 kpc and the circular velocity at the Sun's position ($v_{\rm LSR}$) to be 220 km s^{-1}. We also discuss the effect of changing the value of $v_{\rm LSR}$. The values for the peculiar motion of the Sun (U, V, W)$_\odot$ = (+11.1, +12.24, +7.25) in km s^{-1} are adopted from Schönrich et al. (2010).

Using Equation 3, we can express the log-likelihood function as follows

$$\mathcal{L}(\sigma_r,\sigma_\theta,\sigma_\phi,v_{\rm rot}) = \sum_i^n \log F(l_i,b_i,d_i,v_{los_i}), \quad (4)$$

where n is the total number of stars. Next we use the Markov Chain Monte Carlo (MCMC) to compute the posterior distribution of the model parameters. The median values of the model parameters are quoted as our estimates, whereas 16$^{\rm th}$ and 84$^{\rm th}$ percentiles values are used to compute the associated uncertainties. Note, in the GVE DF (Equation 2), the density term $\rho(r)$ is not a function of the model parameters and thus has no effect on the likelihood analysis.

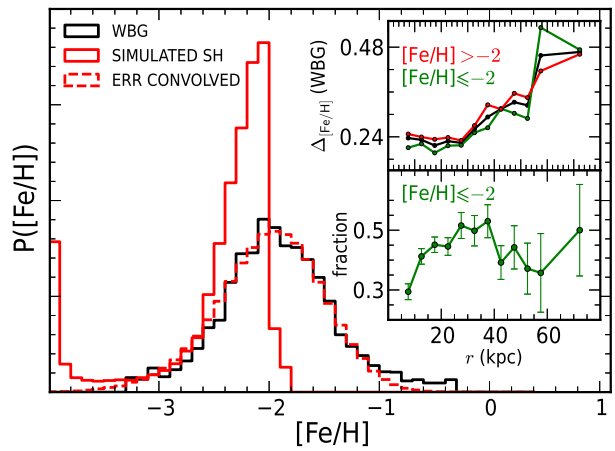

Figure 1. [Fe/H] distribution: Top-inset shows the error in WBG [Fe/H], quoted in the SEGUE database, and the bottom-inset shows the fraction of metal-poor stars with Poisson errors, both as a function of r. In the main plot, the black solid line is the [Fe/H] distribution of our sample, whereas the red solid line is the [Fe/H] distribution of the simulated stellar halo. The red dashed line is the convolved red line (for [Fe/H]> -3.5) with the systematic error of 0.30 and the gaussian random error of 0.40.

2.2 Sample

BHB stars are luminous and their distances can be measured with relatively more accuracy compared to other stellar populations, hence we use them to study the stellar halo. The sample of BHB stars that we use is taken from Xue et al. (2011, X11) comprising 4985 BHB stars obtained from *SDSS/SEGUE*. To minimize contamination from disk stars, we select stars that are well removed from the plane of the disk ($|z| > 4$ kpc). We do not impose any kinematic limits to obtain our sample and hence for the purpose of kinematic studies this sample of BHB stars can be considered to be unbiased. To improve the distances, we recalibrate X11 distances using a color-magnitude relation from Deason et al. (2011b). The dispersion in g-band magnitudes of the data results a distance uncertainty of 6 per cent. In the radial velocity measurements, 95 per cent of our sample has an uncertainty of less than 9 km s^{-1}. The final sample size of the BHB stars we use is 4386.

The X11 catalog of BHB stars originally did not provide the corresponding metallicity values. To obtain [Fe/H], we thus cross-check SEGUE database for each star against the X11 sample. The [Fe/H] metallicity we adopt are the estimates based on Wilhelm et al. (1999) which is provided in the SEGUE database under the heading 'feh_WBG'. In Figure 1, we present the [Fe/H] distribution of our sample. In the inset of the figure, the errors in

WBG [Fe/H] estimates are shown as a function of distance (r) for both the metal-rich (red line) and metal-poor (green line) subsample as well as for the total sample (black line). Note, errors in WBG [Fe/H] beyond $r = 35$ kpc are significantly larger (> 0.27 dex). Also shown in the figure as a red line is the metallicity of BHB stars in the simulated stellar halos by Bullock & Johnston (2005) sampled using the code Galaxia (Sharma et al. 2011a). The code Galaxia takes the N-body particles and their given age and metallicity distributions and then uses Padova stellar isochrones to generate stars. A sharp upper cut-off in the metallicity at around [Fe/H] $\approx$ -1.7 can be seen and this constraint comes purely from the theory of stellar evolution. According to the synthetic isochrones used by Galaxia (Padova isochrones), there are no BHB stars with age less than 13 Gyr and metallicity greater than -1.7. In reality, globular clusters and the field stars (Behr 2003) are found to have metal-rich BHB stars. We find that when the simulated BHB stars are convolved with an uncertainty of 0.40 dex and an offset of 0.30 dex we can match the metallicity of the SEGUE BHB stars (dashed red line). The disagreement among the theoretical prediction and the observed metallicities of the BHB stars could possibly be either because the synthetic isochrone do not correctly model the BHB stars or may be because of inaccuracies in the computation of WBG BHB metallicities quoted in SEGUE database.

Also shown in Figure 1 is the fraction of metal-poor stars ([Fe/H] $\leqslant -2$) as a function of radius. It can be seen that the fraction increases with distance suggesting that the inner regions are slightly biased towards being metal enriched. However, in the outer parts, it starts to fall again due to the sharp increase in uncertainty of [Fe/H] at larger distances, e.g., the outer part could be metal-poor but a large uncertainty in [Fe/H] will spuriously classify metal-poor stars as relatively metal enriched.

3 RESULTS: METALLICITY BIASES IN KINEMATICS

We present here our estimates of the model parameters $\sigma_r(r), \sigma_\theta(r), \sigma_\phi(r)$, $\beta(r)$ and $v_{\rm rot}(r)$ in comparatively metal-rich ([Fe/H] $>$ -2) and metal-poor ([Fe/H]$\leqslant$ -2) bins. To compute the kinematic profiles as a function of radius we choose a moving centre scheme for binning. Briefly, in this binning scheme a set of equispaced positions in r are chosen and then at each position an equal number of points ($n_{\rm bin}$) from the central value are used to estimate the velocity dispersions. The number density of stars in r is not uniform and hence we report the mean r of the points in each bin as its final position. It should be noted that the bins are overlapping in this scheme; a detail discussion on associated pros and cons of using the moving centre bins are given in K12.

3.1 Bias in Mean Azimuthal Velocity Profile

We first compute the profile of mean azimuthal velocity ($v_{\rm rot}$ in Equation 2) with $n_{\rm bin} = 600$. The blue markers in Figure 2 show the $v_{\rm rot}$ profiles of the total sample of BHB stars. It can be seen that the $v_{\rm rot}(r)$ profile of the overall population is nearly constant. The bottom panel shows the profiles for the metal-rich and metal-poor sample separately. In the inner region, $r < 18$ kpc, the metal-rich population is found to have a prograde motion of $v_{\rm rot}$ = 10 km s^{-1} which declines slightly in the outer-region and attains null rotation at $r > 20$ kpc. In contrast, the metal-poor population has a substantial retrograde motion of 30 km s^{-1} for $r < 18$ kpc. At larger r, $v_{\rm rot}$ values of the metal-poor population also decrease to about 18 km s^{-1}. Figure 2 is restricted to $r < 32$ kpc as beyond here

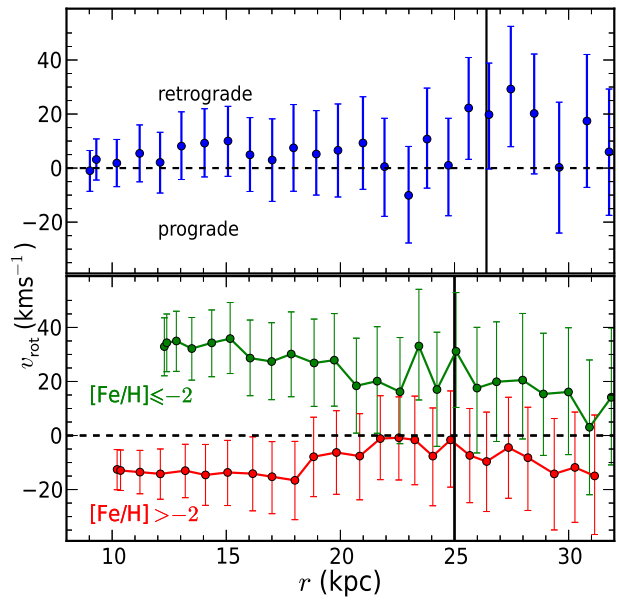

Figure 2. Metallicity bias in $v_{\rm rot}$: $v_{\rm rot}$ estimates in two metallicity bins [Fe/H] > -2 (red) and [Fe/H] $\leqslant -2$ (green). The $v_{\rm rot}$ profile for the total sample is shown with the blue markers. Black vertical solid line demarcates bins that have stars with $r < 30$ kpc.

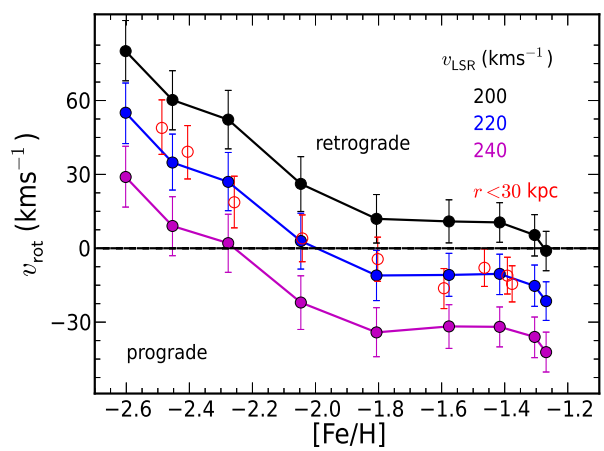

Figure 3. $v_{\rm rot}$ dependence on [Fe/H] and the effect of $v_{\rm LSR}$: The blue dots with the error bars show the $v_{\rm rot}$ as a function of [Fe/H] for the sample of BHB stars, with $v_{\rm LSR}$ = 220 km s^{-1}, whereas red open circles are the values for the sample restricted to $r < 30$ kpc. Black and magenta markers with the error bars are the corresponding estimates for $v_{\rm LSR}$ = 200, 240 km s^{-1} respectively.

the large uncertainty in [Fe/H] (see Figure 1) washes out the distinction between the metal-rich and the metal-poor population and makes the $v_{\rm rot}$ profiles to converge to a common value. Additionally, the error in $v_{\rm rot}$ also begins to increase with r. There are no estimates for metal-poor samples for $r < 12$ kpc which is due to the fewer metal-poor stars in our sample in that regime than the metal-rich stars, as expected.

Deason et al. (2011a) also derive $v_{\rm rot}$ and find that in a large bin ranging $10 < r$ / kpc < 50, the metal-rich population has a net prograde motion of 15 km s^{-1} whereas the metal-poor population

has a net retrograde motion of 25 km s^{-1}. In agreement with Figure 2, it can be said that their estimates of $v_{\rm rot}$ are more likely the better representation of the inner halo within $r < 18$ kpc, but definitely not of the halo out to $r = 50$ kpc. Note that their sample of BHB stars are not selected based on Balmer line-strengths, and thus we anticipate significant contamination from the Blue Straggler population as well as from the cooler and low gravity candidates of the horizontal branch stars (Sirko et al. 2004a) such as RR Lyrae. The fact that the metal-rich and metal-poor profiles do not have a very strong dependence on radius means that we can neglect the radial variation of $v_{\rm rot}$ and study the $v_{\rm rot}$ as a function of metallicity; this is shown in Figure 3. A switch from retrograde to prograde motion at [Fe/H] $\sim$ -1.8 is notable in this figure, suggesting a separate metal-rich component. We checked that this transition also remains for the sub-sample of stars within $r < 30$ kpc, for which errors in [Fe/H] is < 0.27 dex. Given about 0.22 dex uncertainity in [Fe/H], we find that a two component theory, $v_{\rm rot}$ being a step function of [Fe/H], can explain the above profile, but a smooth transition to the low metallicity end cannot be ruled out. From the fact that the $v_{\rm rot}$ profile is not symmetric about [Fe/H] $=$ -2, we can infer that the actual transition to the low metallicity component will be at [Fe/H] $<$ -2. This makes sense in the context of the metallicity distribution of BHB stars for the simulated stellar halo that was shown in Figure 1, namely that the synthetic isochrones predict very few BHB stars with [Fe/H] $>$ -2.

The $v_{\rm LSR}$ has a correlation with $v_{\rm rot}$ estimates. To investigate this we repeat the analysis for different values of $v_{\rm LSR}$ and the results are shown in Figure 3. The effect of changing $v_{\rm LSR}$ is to shift the curves up or down by the corresponding amount but keeping the feature of the profile nearly intact. Hence if $v_{\rm LSR}$ is $\sim$250 km s^{-1} (for $R_\odot = 8.5$ kpc; McMillan & Binney 2010), then the metal-poor population will have nearly zero rotation and the metal-rich population will have a strong prograde rotation. This is consistent with the picture that the metal-poor stars that dominate the outer regions of the halo is formed by accretion of multiple satellites without any preferred direction of rotation. On the other hand, the metal-rich stars that dominate the inner-halo could have their origin related to the disc through the in-situ stars, or due to a massive satellite which happened to have the rotation in the same direction as disc. However, irrespective of the adopted value of $v_{\rm LSR}$, the difference in the rotational properties of metal-rich and metal-poor population remains intact and our results show that the difference in $v_{\rm rot}$ between the most metal-rich and most metal-poor is at least 65 km s^{-1}.

3.2 Bias in Velocity Dispersion Profile

Apart from $v_{\rm rot}$, do the metal-rich and metal-poor subsamples differ in any other kinematic property? To answer this, we study the metallicity dependence of $\sigma_r(r), \sigma_\theta(r), \sigma_\phi(r)$ and $\beta(r)$, and are shown in Figure 4. The dispersions are measured in radials bins with $n_{\rm bin} = 600$ stars for $r < 18.9$ kpc and $n_{\rm bin} = 1200$ for $r > 18.9$ kpc. This demarcation is shown by the vertical dashed line. We have to use larger $n_{\rm bin}$ in the outer parts because fewer stars do not constrain the σ_θ and σ_ϕ. This is because in the outer parts the radial velocity carries less information about the tangential components. A drawback of $n_{\rm bin}$ being large is that the spatial resolution is compromised. Nevertheless, large bins are useful to study general trends. In K12 it was shown that the overall trend in dispersion and β profile of BHB stars remains intact even as $n_{\rm bin}$ is increased from 750 to 1200, except for the fact that the profiles with large $n_{\rm bin}$ are smoothed versions of those with lower $n_{\rm bin}$.

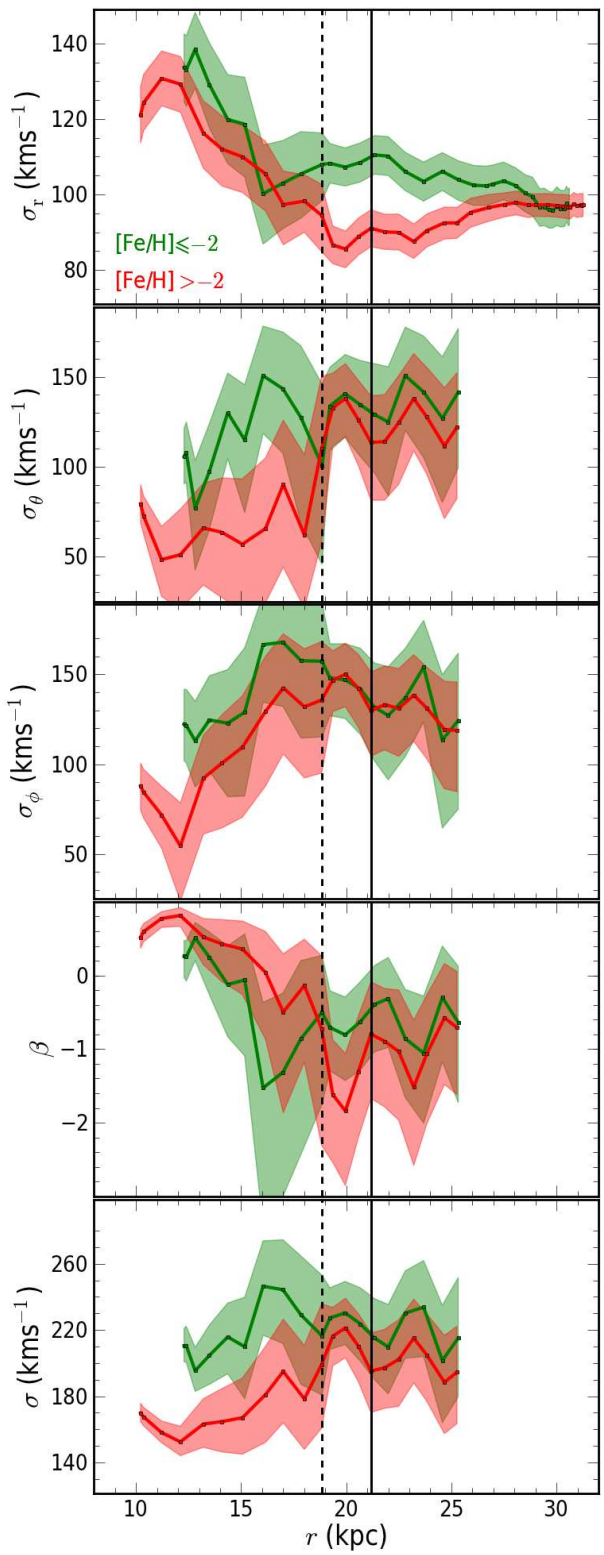

Figure 4. Metallicity bias in the velocity dispersions: red and green lines are the estimated values of velocity dispersions and corresponding β and σ in the comparatively metal-rich ([Fe/H] > -2) and metal-poor ([Fe/H] $\leqslant -2$) bins. Shaded area denote the errors associated.

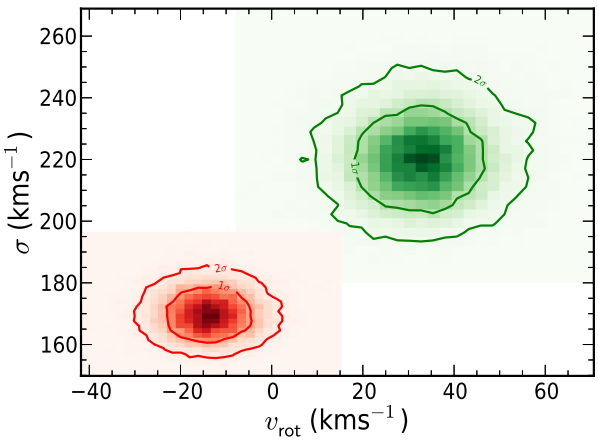

Figure 5. Metallicity bias for the sample in a range $5 < r$/kpc< 20 : the 1σ and 2σ confidence contours for the joint-probability distributions of the parameters in two metallicity bins [Fe/H] > -2 (red) and [Fe/H] $\leqslant -2$ (green) respectively.

From the figure we can see that below $r = 16$ kpc the trends in all the five listed profiles are similar for both the meal-rich and metal-poor populations. Namely, with increase in r, the σ_r decreases, the σ_θ and σ_ϕ increase and the β decreases. However, the profiles are offset from each other. Also, the total dispersion σ $(= \sqrt{(}\sigma_r^2 + \sigma_\theta^2 + \sigma_\phi^2))$ is found to have an offset (40 km s^{-1}). Overall the metal-poor population has lower β than metal-rich. The maximum difference is at $r = 16$ kpc, with σ_θ being very high and the β being very low for the metal-poor population. Going from $r = 16$ to $r = 20$ kpc, one finds that the metal-poor population has almost constant σ_r whereas for the metal-rich population the σ_r drops. The β profile for the metal-poor population remains relatively constant whereas for the metal-rich it keeps on decreasing with minimum value being about -2.

Beyond $r = 20$ kpc, the metal-rich and metal-poor profiles slowly start to converge. This is probably related to the fact that the uncertainty in [Fe/H] increases sharply beyond $r = 30$ kpc. So any kinematic differences between the metal-poor and metal-rich are expected to be washed out if stars beyond $r = 30$ kpc are included. Note in our scheme the bins are overlapping, so a bin at a given radius can contain stars within a wide range in r. To show this more clearly, in the figure we plot a solid vertical line that demarcates bins that have stars with $r < 30$ kpc. It can be seen that as we move to the right of this line the two σ_r profiles start to converge.

The fall at $r = 16$ kpc in σ_r of the metal-rich population roughly coincides with the break radius in the density distribution of the halo stars; this fall was also noticed by Deason et al. (2011a) in the $\sigma_{\rm los}$ profile. In a recent paper (Deason et al. 2013), it was postulated that a break radius in the density profile of a halo could be due to accretion of a massive metal-rich accretion event and a signature of this would be the fall in σ_r of the metal-rich population. We do see this dip in the metal-rich BHB stars but they are found to be on tangential orbits while shell-like structures in the Bullock & Johnston (2005) simulations are generally found for satellites on highly radial orbits. It remains to be seen if a satellite on more milder radial orbit can still give rise to a break in density.

It is apparent in the Figures 2 and 4 that the analyses are done in smaller bin sizes and consequently, the errors for each bin are larger. Thus, here we also provide additional measures of our model parameters, σ, β and $v_{\rm rot}$, for the metal-rich and the metal-poor samples covering the larger radial range $5 < r$/kpc< 20. In Figure 5, we show the joint probability distributions of the model parameters for these sub-samples, where for the metal-poor and the metal-rich samples the confidence contours (1σ and 2σ) are shown in green and red colors respectively. The estimated values of these parameters are given in Table 1. The differences among the estimated values of the kinematic parameters σ and $v_{\rm rot}$ of the metal-rich and the metal-poor samples are found to be $\sim$ 50 km s^{-1}. Also given in Table 1 are the estimates of the parameters for the sample masked to remove the contamination from Sagittarius stellar stream and the Virgo overdensity . The cuts chosen to mask these structures are purely geometrical and are same as given in Section 3.4 of K12 (for the further details about the cuts see the references provided there within). It can be seen in the Table that the exclusions of these two substructures has negligible effect on the final results.

Table 1. Estimated parameters in the comparatively metal-rich and metal-poor bins in the range $5 < r$/kpc< 20 for two different cases namely, when Sagittarius stream and Virgo-overdense region masked and unmasked.

Saggi-Virgo	[Fe/H]	β	σ (kms^{-1})	$v_{\rm rot}$ (kms^{-1})
Unmasked	> -2	$0.3^{+0.1}_{-0.2}$	170^{+6}_{-6}	-14^{+6}_{-6}
Masked	> -2	$0.3^{+0.1}_{-0.2}$	170^{+6}_{-6}	-15^{+6}_{-7}
Unmasked	$\leqslant -2$	$-0.4^{+0.3}_{-0.4}$	220^{+11}_{-11}	33^{+9}_{-10}
Masked	$\leqslant -2$	$-0.4^{+0.3}_{-0.5}$	220^{+12}_{-11}	35^{+10}_{-10}

4 CONCLUSIONS

In this paper, we derived the mean azimuthal velocity, the velocity dispersion and the anisotropy profiles of the Milky Way stellar halo, using BHB stars, as a function of distance r and metallicity [Fe/H].

The comparatively metal-rich ([Fe/H] $>$ -2) and metal-poor ([Fe/H] $\leqslant$ -2) populations of BHB stars within $r < 16$ kpc have distinct kinematic properties with offsets of 40 km s^{-1} in both $v_{\rm rot}$ and σ. Additionally, an offset is also found in σ_r, σ_θ, σ_ϕ and β. This suggests the presence of at least two sub-populations in the halo. When $v_{\rm rot}$ is studied as a function of [Fe/H], we find that $v_{\rm rot}$ decreases monotonically and then saturates to a constant value for [Fe/H] > -1.8. The saturation again suggests the existence of a distinct metal-rich component. The difference in rotation between the most metal-poor and most metal-rich population was found to be around 65 km s^{-1}.

Overall the β profile for both the metal-rich and the metal-poor populations show similar trends with radius, i.e., β decreases with radius and then saturates at a negative value. This is in agreement with Deason et al. (2011a) in the sense that β is more a function of radius than metallicity, but differs slightly from C07 who suggest that the metal-rich halo is radial while the metal-poor has a wide range of values of β. Our results suggest that below $r < 15$ kpc, the metal-rich population has radial orbits and the metal-poor population is on average tangential. But in the range $15 < r$/kpc < 25, both the metal-rich and metal-poor populations are predominantly tangential. Finally, regarding the spatial distribution of the metallicity we find that although the inner regions ($r < 15$ kpc) are slightly biased towards being metal-rich, in general the metal-rich and metal-poor populations have substantial spatial overlap.

There are two factors which make it difficult to compare the BHB results with the findings of C07. Firstly, BHB stars are in general metal-poor so they preferentially sample the metal-poor population of the halo. Secondly, there is significant uncertainty in estimated metallicity. The uncertainty in fact increases sharply beyond 30 kpc. The above two factors will lead to significant overlap between the metal-poor and metal-rich populations and will smooth out the differences between the two populations. We do find evidence of this in the outer parts ($r > 25$ kpc) where a convergence in σ_r and $v_{\rm rot}$ is noticed for the distinct populations due to the larger measurement uncertainties. Thus the physical differences between the two populations could be even stronger, but a deeper stellar survey would be required to confirm this.

Note a contamination of the BHB stars with other populations still a possibility. We find that theoretical isochrones do not predict BHB stars with [Fe/H] > -1.7 and have ages less than 13 Gyr. A distribution of synthetic BHB stars can only be matched if we convolve with an uncertainty of 0.40 dex and allow for an offset of 0.30 dex with respect to the metallicity of the SEGUE BHB stars. However, some probable field BHB stars (e.g. BD+49°2137 from Behr (2003)) have been found to be metal-rich, thus it could be true that the synthetic isochrone do not model BHB stars well. Within r =16-20 kpc, we find that the σ_r and β of the metal-rich population decrease sharply while that of the metal-poor population show a slight increase. The fall in σ of the metal-rich population roughly coincides with the break radius in the density distribution of the halo stars. As suggested by Deason et al. (2013) this could be a signature of accretion of a massive metal-rich accretion event.

To conclude, we find that the metal-rich and the metal-poor populations of the halo BHB stars have distinct differences in kinematic properties. But note that there is no sharp transition from one population to another e.g. C07 [Fe/H] distributions of the inner-halo and the outer-halo peak at -1.6 and -2.2 respectively but have a spread which are larger than the difference of their peak values. Therefore a simple division into two groups by [Fe/H] will include substantial numbers of the outer-halo in the metal-rich group and vice-versa.

The difference in the metal-rich and metal-poor seen by us is in qualitative agreement with earlier observational findings of C07, Carollo et al. (2010), and Deason et al. (2011a) and supports the dual formation scenario as seen in cosmological simulations, i.e., the inner halo is dominated by an in-situ component and the outer halo by an accreted component (e.g., Zolotov et al. 2009; Font et al. 2011; McCarthy et al. 2012). However, to accept or reject the above hypothesis, a detailed comparison of observations with simulations still needs to be done. Also a comparative study of the kinematics of stellar populations other than BHB stars such as turn-off stars (fairer sample in metallicity) or giants (probing farther region of the outer-halo) or standard candles e.g. RR Lyrae (accurate distances) is needed.

ACKNOWLEDGEMENTS

P.R.K acknowledges University of Sydney International Scholarship for the support of his candidature. G.F.L acknowledges support from ARC Discovery Project (DP110100678) and Future Fellowship (FT100100268). J.B.H. is funded through a Federation Fellowship from the ARC and S.S. is funded through ARC DP grant 0988751 which supports the HERMES project. We sincerely thank the anonymous referee for comments that helped to improve the paper.

REFERENCES

Beers T. C. et al., 2012, ApJ, 746, 34
Behr B. B., 2003, ApJS, 149, 101
Bell E. F. et al., 2008, ApJ, 680, 295
Belokurov V. et al., 2006, ApJL, 642, L137
Binney J., Tremaine S., 2008, Galactic Dynamics: Second Edition. Princeton University Press
Bond N. A. et al., 2010, ApJ, 716, 1
Bullock J. S., Johnston K. V., 2005, ApJ, 635, 931
Carollo D. et al., 2007, Nature, 450, 1020
Carollo D. et al., 2010, ApJ, 712, 692
Deason A. J., Belokurov V., Evans N. W., 2011a, MNRAS, 411, 1480
Deason A. J., Belokurov V., Evans N. W., 2011b, MNRAS, 416, 2903
Deason A. J., Belokurov V., Evans N. W., Johnston K. V., 2013, ApJ, 763, 113
Font A. S., McCarthy I. G., Crain R. A., Theuns T., Schaye J., Wiersma R. P. C., Dalla Vecchia C., 2011, MNRAS, 416, 2802
Freeman K., Bland-Hawthorn J., 2002, ARA&A, 40, 487
Frenk C. S., White S. D. M., 1980, MNRAS, 193, 295
Gilbert K. M., Font A. S., Johnston K. V., Guhathakurta P., 2009, ApJ, 701, 776
Helmi A., 2008, A&AR, 15, 145
Ibata R. A., Gilmore G., Irwin M. J., 1995, MNRAS, 277, 781
Kafle P. R., Sharma S., Lewis G. F., Bland-Hawthorn J., 2012, ApJ, 761, 98
Majewski S. R., 1993, ARA&A, 31, 575
McCarthy I. G., Font A. S., Crain R. A., Deason A. J., Schaye J., Theuns T., 2012, MNRAS, 420, 2245
McMillan P. J., Binney J. J., 2010, MNRAS, 402, 934
Schönrich R., Binney J., Dehnen W., 2010, MNRAS, 403, 1829
Schönrich R., Asplund M., Casagrande L., 2011, MNRAS, 415, 3807
Sharma S., Bland-Hawthorn J., Johnston K. V., Binney J., 2011a, ApJ, 730, 3
Sharma S., Johnston K. V., Majewski S. R., Bullock J., Muñoz R. R., 2011b, ApJ, 728, 106
Sirko E. et al., 2004a, AJ, 127, 899
Sirko E. et al., 2004b, AJ, 127, 914
Smith M. C., Wyn Evans N., An J. H., 2009a, ApJ, 698, 1110
Smith M. C. et al., 2009b, MNRAS, 399, 1223
Starkenburg E. et al., 2009, ApJ, 698, 567
Tissera P. B., White S. D. M., Scannapieco C., 2012, MNRAS, 420, 255
Wilhelm R., Beers T. C., Gray R. O., 1999, AJ, 117, 2308
Xue X. X. et al., 2011, ApJ, 738, 79
Zolotov A., Willman B., Brooks A. M., Governato F., Brook C. B., Hogg D. W., Quinn T., Stinson G., 2009, ApJ, 702, 1058